European Journal of Neuroscience, Vol. 19, pp. 2997–3005, 2004

Brain virus burden and indoleamine-2,3-dioxygenase expression during lentiviral infection of rhesus monkey are concomitantly lowered by 6-chloro-2′,3′-dideoxyguanosine

Candan Depboylu,[1,2] Todd A. Reinhart,[3] Osamu Takikawa,[4] Yoshinori Imai,[5] Hitomi Maeda,[6] Hiroaki Mitsuya,[6] Dianne Rausch,[7] Lee E. Eiden[7] and Eberhard Weihe[1]
[1]Department of Molecular Neuroscience, Institute of Anatomy and Cell Biology, Philipps University, Marburg, Germany
[2]Department of Neurology, Philipps University, Marburg, Germany
[3]Department of Infectious Diseases and Microbiology, University of Pittsburgh, Pittsburgh, USA
[4]Department of Molecular Biochemistry, Central Research Institute, School of Medicine, Hokkaido University, Sapporo, Japan
[5]Department of Neurochemistry, National Institute of Neuroscience, Tokyo, Japan
[6]Experimental Retrovirology Section, HIV and AIDS Malignancy Branch, Center for Clinical Research, NCI, NIH, Bethesda, USA
[7]Section on Molecular Neuroscience, Laboratory of Cellular and Molecular Regulation, NIMH, NIH, Bethesda, USA

Keywords: antiretroviral, kynurenine pathway, microglia/ macrophage, neuroinflammation, quinolinic acid

Abstract

Increased kynurenine pathway metabolism has been implicated in the aetiology of lentiviral encephalopathy. Indoleamine-2,3-dioxygenase (IDO) initiates the increased production of kynurenine pathway metabolites like quinolinic acid (QUIN). QUIN itself is elevated in AIDS-diseased monkey and human brain parenchyma and cerebrospinal fluid at levels excitotoxic for neurons *in vitro*. This study investigates the cellular origin of IDO biosynthesis in the brain of rhesus monkeys infected with simian immunodeficiency virus (SIV) and explores the effects of CNS-permeant antiretroviral treatment. IDO transcript and protein were absent from the brain of non-infected and SIV-infected asymptomatic monkeys. IDO biosynthesis was induced in the brain of monkeys exhibiting AIDS. Nodule and multinucleated giant cell-forming macrophages were the main sources of IDO synthesis. Treatment with the lipophilic 6-chloro-2′,3′-dideoxyguanosine suppressed IDO expression in the brain of AIDS-diseased monkeys. The effectiveness of this treatment was confirmed by the reduction of virus burden and SIV-induced perivascular infiltrates, mononuclear nodules and multinucleated giant cells. Our data demonstrate that brain IDO biosynthesis is induced in a subset of monocyte-derived cells, depends on viral burden and is susceptible to antiretroviral treatment. Thus, IDO induction is associated with reversible overt inflammatory events localized to areas of active viral replication in the SIV-infected brain.

Introduction

Macaques infected with simian immunodeficiency virus (SIV) develop cognitive and motor dysfunctions like human immunodeficiency virus (HIV)-infected individuals (Murray *et al*., 1992). Impairments occur with low or marked encephalitis characterized by astrogliosis, nodule and giant cell formation, infiltrates, myelin pallor and vessel leakage (Budka, 1986; Lane *et al*., 1986; Weihe *et al*., 1993; Luabeya *et al*., 2000). Loss of synapses, dendrites and neurons also occur in SIV disease (Luthert *et al*., 1995; Li *et al*., 1999; Bissel *et al*., 2002). Neurodegenerative damage could be caused by virus-derived or host-derived neurotoxic products or by a combination of both (Lipton *et al*., 1991; Li *et al*., 1999), resulting in dementia in HIV-infected patients (Lawrence & Major, 2002). One of these host-generated toxins is quinolinic acid (QUIN). QUIN stimulates *N*-methyl-D-aspartate (NMDA)-type glutamate receptors (Perkins & Stone, 1983) and releases glutamate itself (Tavares *et al*., 2002). QUIN elevation presumably contributes to altered neuronal activity (Abele *et al*., 1990), neurodegeneration (Schwarcz *et al*., 1983), other neurochemical alterations (Beal *et al*., 1989) and astrogliosis (Block & Schwarz, 1994) in neuro-AIDS. Due to regional differences of NMDA-receptor distribution, some brain regions and neuronal populations are more vulnerable to the neurotoxic effect of QUIN than others (Schwarcz & Köhler, 1983).

The rate-limiting enzyme indoleamine-2,3-dioxygenase (IDO) catalyses the conversion of L-tryptophan into L-kynurenine. Subsequent enzymatic and non-enzymatic reactions convert L-kynurenine to QUIN. IDO is induced by cytokines, particularly interferon-γ released during systemic or brain inflammatory processes (Takikawa *et al*., 1988; Dai & Gupta, 1990). Increased brain QUIN is directly related to IDO induction (Heyes *et al*., 1988, 1989). It is hypothesized that QUIN in the brain comes from glial elements, endothelial cells, activated microglia and blood-derived macrophages (Brew *et al*., 1995; Heyes *et al*., 1997; Guillemin *et al*., 1999; Hansen *et al*., 2000). In the periphery, IDO was found to be expressed in dendritic cells and to influence lymphocyte function (Mellor *et al*., 2002; Munn *et al*., 2002). However, the sites of IDO expression during brain inflammation are not clearly identified in viral inflammatory diseases, limiting further understanding of the role of IDO-generated neurotoxins in neuro-AIDS and other neurodegenerative and neuroinflammatory diseases.

Correspondence: Dr E. Weihe, as above.
E-mail: weihe@staff.uni-marburg.de

Received 13 November 2003, revised 18 March 2004, accepted 19 March 2004

doi:10.1111/j.1460-9568.2004.03404.x

This study aims to determine if, where and how IDO is synthesized and regulated in SIV-induced brain inflammatory disease. Additionally, the influence of a lipophilic antiretroviral agent on brain IDO expression was analysed.

Materials and methods

Virus stock and inoculation procedures in rhesus monkeys

Juvenile rhesus macaques were housed in the BIOQUAL animal facility (Rockville, MD, USA), which is fully accredited by the American Association for Accreditation of Laboratory Animal Care. They were determined negative for simian retrovirus-1 and -2, SIV and simian herpes virus. Animals were inoculated intravenously with 10 rhesus infectious doses of cell-free $SIV_{\delta B670}$ grown in human peripheral blood mononuclear cells. Virus was obtained as an aliquot of a previously characterized virus stock stored in liquid nitrogen (da Cunha *et al*., 1995). Following inoculation, animals were monitored and examined for clinical evidence of disease. In short intervals blood and cerebrospinal fluid (CSF) samples were obtained from the animals. At time of killing and necropsy eight macaques exhibited clinical signs of AIDS and five did not. AIDS-defining criteria included one or more of the following: loss of body weight over 10%, intractable diarrhoea/dehydration requiring fluid replacement, oral lesions/thrush and other opportunistic infections. Four age-matched non-infected macaques were used as controls. Experiments involving the use of rhesus macaques were approved by the Animal Care and Use Commitee of Bioqual, Inc., an NIH-approved and Association for Assessment and Accreditation of Laboratory Animal Care (AAALAC)-accredited research facility. All experiments were carried out using the ethical guidelines promulgated in the National Institutes of Health Guide for the Care and Use of Laboratory Animals.

Antiretroviral treatment

Four SIV-infected monkeys, in which the viral load was found to be >100,000 virions/mL in plasma and >100 virions/mL in CSF in more than two consecutive examinations underwent treatment with 2′,3′-dideoxyinosine (ddI) or 6-chloro-2′,3′-dideoxyguanosine (6-Cl-ddG) subcutaneously (Shirasaka *et al*., 1990, 1991; Hawkins *et al*., 1995), and were killed shortly thereafter. These monkeys developed signs of AIDS-defining criteria during the course of antiretroviral treatment until death. Three of these four monkeys (MO76, MO77 and MO91) received 10 mg/kg/day ddI for 3 weeks for clinical stabilization and then 75 mg/kg/day of 6-Cl-ddG for 6 weeks. The fourth monkey (MO89) received 6-Cl-ddG (200 mg/kg/day) for 3 weeks. The vehicle for ddI administration was phosphate-buffered saline (PBS) and for 6-Cl-ddG administration 70% propylene glycol/30% PBS.

Tissue preparation for histochemical analysis

Prior to killing, animals were anaesthetized with ketamine (20 mg/kg) and ketamine-acepromazine (10 mg/kg), then perfused transcardially in the following sequence: PBS, 1% formalin/PBS and 4% formalin/PBS. Tissue specimens were obtained at necropsy and immersion-fixed overnight in 4% paraformaldehyde/PBS. Some blocks were cryopreserved in 10–20% sucrose/PBS over 48 h and snap frozen in cooled isopentane. Some blocks were postfixed in Bouin–Hollande solution, followed by extensive washes in 70% 2-propanol, dehydration and processing for paraffin embedding.

Radioactive and non-radioactive in situ *hybridization (ISH) histochemistry*

[^{35}S]-UTP- and digoxigenin-UTP-labelled human specific sense and antisense orientated riboprobes were generated by *in vitro* transcription

TABLE 1. Compiled results at time of killing and necropsy

Monkey number	Duration of infection (months)	Drug treatment*	Brain SIV burden†	Degree of SIV-induced encephalitis‡	Brain IDO synthesis§	Clinical findings
44	Not infected	Not treated	–	–	–	No disease
50	Not infected	Not treated	–	–	–	No disease
69	Not infected	Not treated	–	–	–	No disease
87	Not infected	Not treated	–	–	–	No disease
75	2.5	Not treated	–	–	–	Asymptomatic
80	6.5	Not treated	–	–	–	Asymptomatic
85	4.5	Not treated	–	–	–	Asymptomatic
92	6.0	Not treated	–	–	–	Asymptomatic
93	4.5	Not treated	–	–	–	Asymptomatic
46	19.0	Not treated	+	+	+	Diarrhoea, mycotic infection, mass
71	6.5	Not treated	++	++	++	Diarrhoea, listless, rash
74	6.0	Not treated	+++	+++	++	Diarrhoea, anaemia, parasitic infection, LN atrophy
78	2.4	Not treated	+++	+++	+++	Diarrhoea, parasitic infection, pneumonitis
79	2.5	Not treated	+	+	+	Rash, heart murmur, LN atrophy
82	3.0	Not treated	+++	+++	+++	Diarrhoea, wasting
86	4.5	Not treated	+++	+++	++	Wasting, mass, thrush, colitis, LN atrophy
90	2.3	Not treated	++	++	++	Vomiting, wasting, tube feed
76	22.0	ddI/6-Cl-ddG	–	–	–	Wasting, diarrhoea, heart murmur, anaemia
77	4.0	ddI/6-Cl-ddG	+/–	+/–	+/–	Incontinence, wasting, diarrhoea
89	22.0	6-Cl-ddG	–	–	–	Anaemia, wasting, diarrhoea, lymphoma
91	6.1	ddI/6-Cl-ddG	–	–	–	Wasting, diarrhoea

*Treatment with ddI prior with the CNS-permeant 6-Cl-ddG; MO89 received only 6-Cl-ddG. †Detection of SIV env/pol by ISH; detection of SIV *gp120* by IHC. ‡SIV-induced mononuclear reactions monitored by IHC for Iba1, scoring was as: +++ for severe, ++ for moderate and + for mild SIV-induced encephalitis with appearance of macrophage nodules, mononuclear cell infiltrates, multinucleated giant cells, – for no SIV-induced encephalitis. §Detection of IDO mRNA by ISH and of IDO protein by IHC; IHC for SIV *gp120* and IDO as well as ISH for IDO and SIV were scored as: – (no immunoreactive cells or cells with more than background silver grains) to +++ (>100 immunoreactive cells or cells with significantly greater number of silver grains than background per mm^2); numbers are not specifically determined; sections from temporal cortex, hippocampus and basal ganglia were analysed and summarized. 6-Cl-ddG, 6-chloro-2′,3′-dideoxyguanosine; ddI, 2′,3′-dideoxyinosine; IDO, indoleamine-2,3-dioxygenase; LN, lymph node; SIV, simian immunodeficiency virus.

from linearized pBluescript KS+ containing human IDO (accession no: M34455; kindly provided by S. L. Gupta, Hipple Cancer Research Center, Dayton, USA; Dai & Gupta, 1990) and alkaline hydrolysed to 200–250 nucleotide fragments prior to application. For prehybridization, frozen cryopreserved tissue sections (14 μm) were incubated in 10 mM Na-citrate buffer (pH 6.0) at 95 °C for 15 min, washed in PBS and in 0.4% Triton X-100/PBS for 10 min, acetylated with triethanolamine/acetic-anhydride (pH 8.0) for 10 min, rinsed in distilled water, dehydrated in graded ethanols, dried and used for hybridization, or stored at −20 °C until use. Hybridization with cRNA probes diluted in hybridization mix (final concentration of 50×10^3 d.p.m./μL for radioactive probe and 1 ng/μL for non-radioactive probe) overnight at 60 °C and post-hybridization were carried out as described previously (Schäfer *et al*., 1992). Radioactive hybridization signals were revealed by autoradiography after 2–3 weeks of exposure on slides dipped in NTB-2 emulsion (Eastman Kodak, NY, USA). Non-radioactive hybridization signals were detected according to the manufacturer's instructions (Boehringer, Germany), resulting in a dark blue reaction product. ISH signals were analysed with the Olympus AX70 microscope (Olympus Optical, Germany). Sections from frontal cortex, parietal cortex, temporal cortex, occipital cortex, hippocampus, basal ganglia, thalamus, brainstem and spinal cord were analysed.

Single enzymatic immunohistochemistry (IHC)

As described previously (Weihe *et al*., 1993), IHC was performed on deparaffinized paraffin-embedded tissue sections (7 μm) or cryosec-

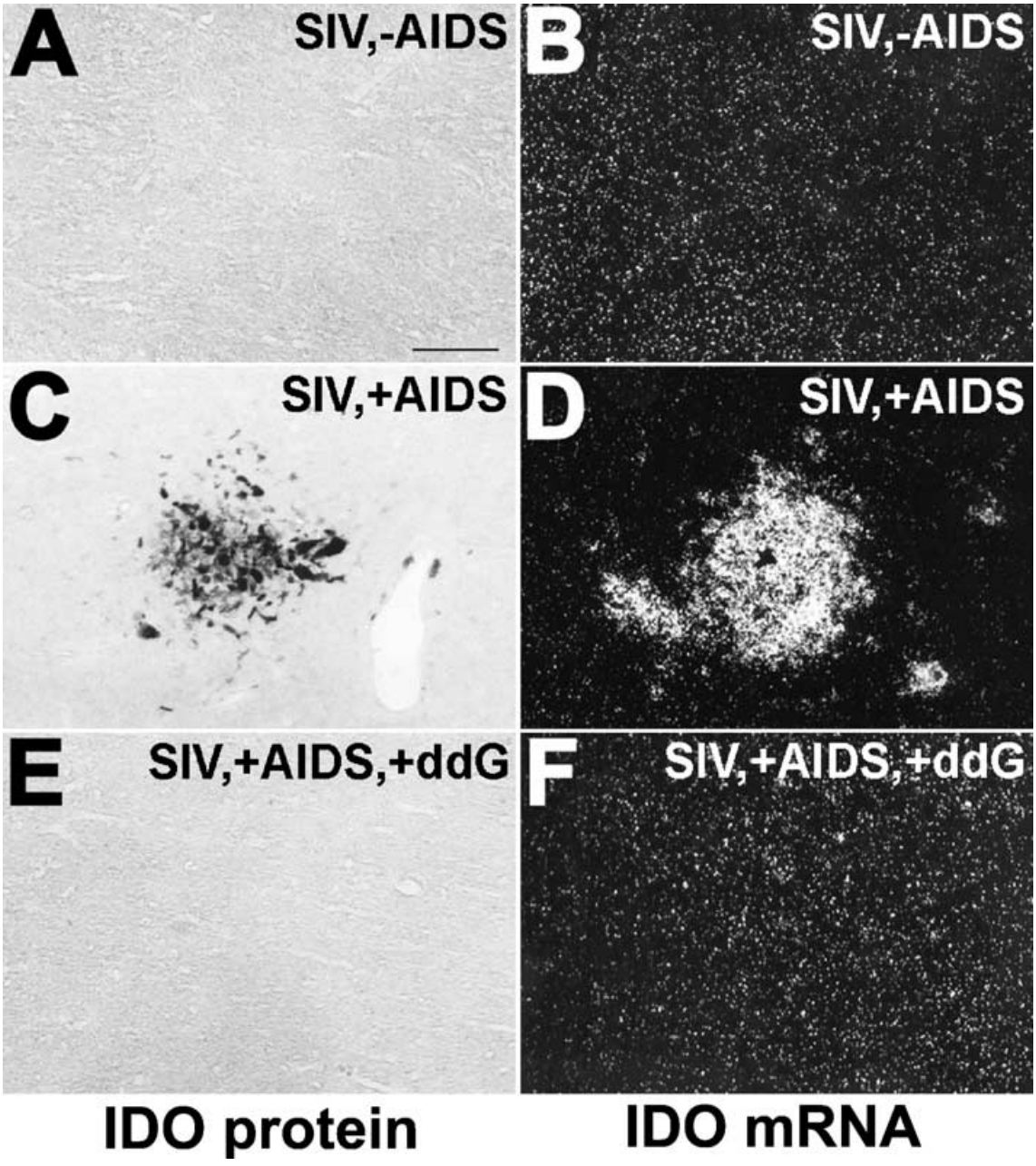

FIG. 1. Indoleamine-2,3-dioxygenase (IDO) biosynthesis in the rhesus monkey CNS in early and late stage of simian immunodeficiency virus (SIV) infection, and effect of antiretroviral treatment. (A, C and E) IHC for IDO protein, (B, D and F) ISH for IDO mRNA. (A and B) IDO protein and transcript are not detected in the brain of SIV-infected monkeys without AIDS (SIV, –AIDS). (C and D) In the brain of untreated SIV-infected monkeys with AIDS (SIV, +AIDS) IDO was induced. 6-Chloro-2′,3′-dideoxyguanosine (6-Cl-ddG) treatment (SIV, +AIDS, +ddG) inhibits expression of IDO protein and mRNA in the brain (E and F). Scale bar, 100 μm (A).

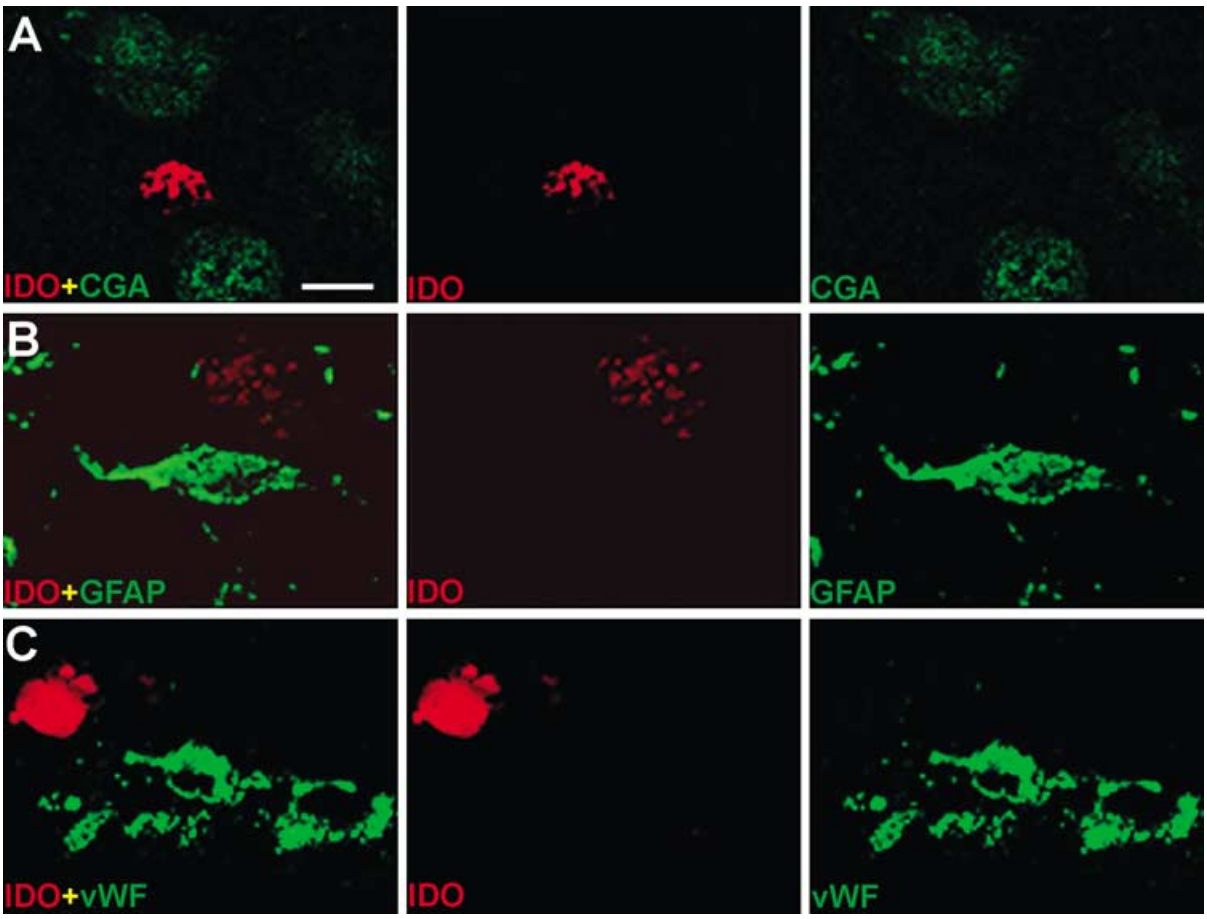

FIG. 2. Confocal laser scanning analysis after double immunofluorescence for IDO with established markers for brain resident cells demonstrates that chromogranin A (CGA)-positive neuronal cell bodies (A), glial fibrillary acid protein (GFAP)-positive astrocytes (B) and von Willebrand factor (vWF)-stained endothelial cells (C) are strictly lacking IDO in SIV encephalitis. Note vesicular appearance of IDO. Singular colours merged at A, B and C. Scale bar, 10 μm (A).

tions (14 μm) using standard avidin–biotin–peroxidase techniques (Vectastain Elite ABC kit, Boehringer). For optimal antigen retrieval, sections were incubated in a pressure cooker (15 min at 95 °C in 10 mM Na-citrate buffer, pH 6.0) and blocked by successive 30-min incubation in bovine serum albumin (BSA) and Avidin-Biotin-Blocking kit (Vectastain Elite, Boehringer). Cells of mononuclear origin were visualized with a rabbit-polyclonal antibody against ionized calcium-adapter binding molecule (Iba1; 1 : 3000; Imai *et al.*, 1996). IDO antigen was detected with a mouse-monoclonal antibody (1 : 400; Takikawa *et al.*, 1988). Primary antibodies were applied in 1%

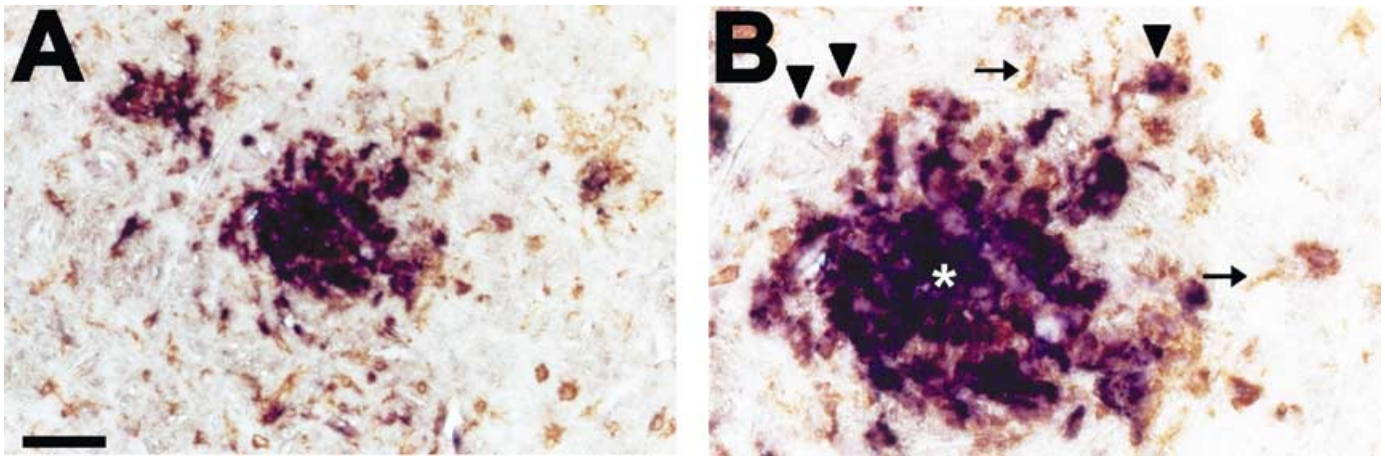

FIG. 3. Combination of non-radioactive ISH for IDO (dark blue reaction product) with cytochemistry for Iba1 (brown reaction product) on a brain section of an AIDS-diseased monkey. IDO mRNA is mainly localized in Iba1-positive macrophages and giant cell in the nodule (asterisk) but also in some Iba1-positive perinodular cells with mostly non-ramified appearance (arrow heads). Note also the presence of Iba1-positive cells with the appearance of ramified microglia, which are devoid of hybridization signals for IDO (arrows). Scale bar, 100 μm (for A); 50 μm (for B).

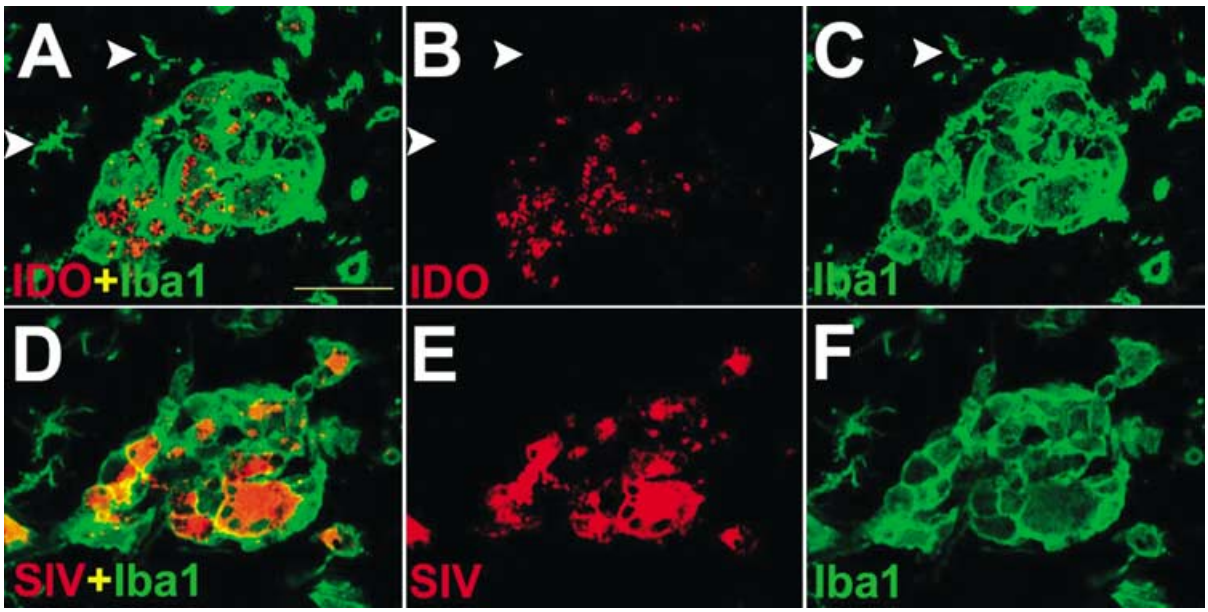

FIG. 4. Confocal double immunofluorescence of adjacent sections of a nodule from an AIDS-diseased monkey alternately stained for IDO with ionized calcium-adapter binding molecule (Iba1; A–C) and for SIV *gp120* with Iba1 (D–F), respectively. Note overlap of the distribution of IDO-positive and SIV-positive cells (B and E). Both IDO- and SIV-positive cells coincide with Iba1 within the nodule (C and F). Note distribution of Iba1 immunoreactivity to the surface of the nodular cells, while IDO and SIV immunoreactivities are localized to cell cytoplasm. Iba1-positive microglial cells in the perinodular region (arrow heads) lack immunoreactivity for IDO. Scale bar, 20 μm (A).

BSA/PBS and incubated at 16 °C overnight followed by 3 h at 37 °C. Sections were washed and incubated with species-specific biotinylated IgG from donkey (1 : 200; Dianova, Germany) for 1 h at 37 °C. Immunoreactions were visualized with 3,3′-diaminobenzidine (Sigma, Germany), resulting in a brown staining, or enhanced with 0.08% Nickel-salt (Fluka, Switzerland), resulting in a dark blue staining. IHC signals were analysed with the Olympus AX70 microscope (Olympus Optical).

Dual colour immunofluorescence and confocal laser scanning analysis

IDO and Iba1 were detected with the antibodies from mouse and rabbit at 1 : 40 and 1 : 300 dilutions, respectively. IDO was visualized by incubation with mouse-specific indocarbocyamine- or Alexa 647-conjugated IgG (1 : 100; Dianova), resulting in red-orange fluorescence labelling. Iba1 was detected after incubation with rabbit-specific biotinylated IgG and then with Alexa 488-conjugated streptavidin (1 : 200; MoBiTec, Germany), resulting in green fluorescence. The $SIV_{\delta B670}$ was visualized with a cross-reacting mouse-monoclonal antibody KK45 against SIV_{mac251} glycoprotein 120 (*gp120*; 1 : 200; NIH AIDS Research & Reference Program, USA) and with Alexa 647-conjugated antimouse IgG (Kent *et al*., 1992). Neurons were visualized with a rabbit-polyclonal antichromogranin A (CGA) antibody (1 : 1000; Schäfer *et al*., 1994), endothelial cells with a rabbit-polyclonal anti-von Willebrand factor (vWF) antibody (1 : 500 diluted; DAKO, Germany; Theilen & Kuschinsky, 1992) and astrocytes with a polyclonal anti-glial fibrillary acid protein (GFAP) guinea pig-antibody (1 : 400; Progen, Germany; Weihe *et al*., 1993). All three cell types were detected with Alexa 488-conjugated streptavidin after incubation with species-specific biotinylated IgG (1 : 200; Dianova). To make definitive statements of coexistence and non-coexistence pattern of IDO in neurons, astrocytes and endothelial cells in representative sections, containing hundreds to thousands of cells identified by the appropriate markers, we examined several sections (up to three) from several brain regions and for each untreated AIDS-diseased animal. Fluorescence signals were documented with the Olympus Fluoview confocal laser scanning microscope (Olympus Optical).

Combination of non-radioactive ISH with enzymatic IHC

For visualizing antigen with an RNA transcript in the same tissue section, IHC was performed in combination with ISH. Prehybridization, hybridization with the DIG-labelled probe against IDO mRNA and post-hybridization were performed as described. DIG-ISH signals

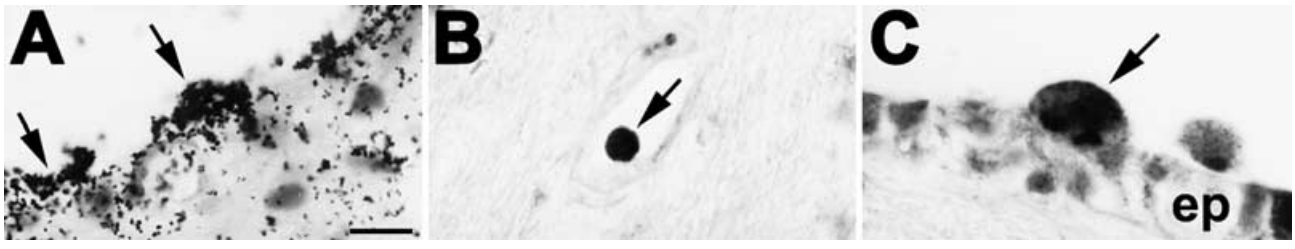

FIG. 5. Cells expressing IDO at the brain barrier of an untreated monkey with AIDS. (A and B) IDO transcript and protein-expressing monocytes (arrows) are attached to the endothelium surface. (C), IDO-positive multinucleated giant cell (arrow) is lying on the ependymal surface (ep). Scale bar, 12.5 μm (A).

for IDO mRNA were detected, resulting in a purple blue reaction product. After that Iba1 was visualized by 3,3′-diaminobenzidine-IHC as described, resulting in a brown reaction product. The reaction products could clearly be differentiated at the cellular level.

Detection of viral burden

For analysis of viral transcription, ISH was performed using probes generated by incorporation of [^{35}S] into SIV RNA probes by *in vitro* transcription of SIV_{mac239} sequences cloned in a pTRIKAN19 vector, or into DNA probes by random priming using sequences of cloned $SIV_{macBK28}$ DNA (Reinhart *et al*., 1997). Activities of radioactive probes were $30–50 \times 10^3$ d.p.m./μL. The DNA templates were a *KpnI* fragment from the *pol* gene of SIV_{mac239} (nucleotide positions 5208–4713) or a *BamHI* fragment from $SIV_{macBK28}$ (nucleotide positions 1841–9174). In some experiments, ISH was performed with oligonucleotides specific for unspliced SIV RNA complementary to sequences at the exon/intron junction at the 5′-end of unspliced RNA (nucleotide positions 996–967of SIV_{smH4} proviral sequence) as described by Reinhart *et al*. (1997). The sequences in the control sense probe were identical to sequences at the same exon/intron junction (nucleotide positions 967–996 of SIV_{smH4}). Polyacrylamide gel-purified nucleotides were 3′-end-labelled with [^{35}S]-dCTP using terminal deoxynucleotide transferase to specific activities of $2–8 \times 10^9$ cpm/μg. For ISH, slide-mounted sections (14 μm) of cryopreserved tissues were postfixed in 4% paraformaldehyde/PBS, washed and dehydrated. Pretreatments consisted of incubation for 20 min each in 0.2 N HCl at ambient temperature; 2 × SSC at 70 °C; and 2 mM $CaCl_2$, 20 mM Tris (pH 7.5) and 10 μg/mL proteinase K at 37 °C, followed by washing, acetylation and dehydration. Sections were then hybridized for 18 h at 45 °C (for riboprobes) or at 37 °C (for oligonucleotide probes). After post-hybridization sections were coated with NTB-2 emulsion and exposed at 4 °C for 3–6 days. After development, the sections were counterstained with cresyl violet. Sections from frontal cortex, parietal cortex, temporal cortex, hippocampus, basal ganglia, thalamus, brainstem and spinal cord were analysed.

Results

Analysis of IDO protein and transcript expression was performed on brain tissue sections of uninfected control monkeys (Ctrl), SIV-infected monkeys without AIDS (SIV, –AIDS) and SIV-infected monkeys exhibiting AIDS (SIV, +AIDS). A fourth group consisted of monkeys with high viremia and increased viral load in CSF at initiation of antiretroviral treatment and suffering from AIDS (SIV, +AIDS, +ddG). All animals are summarized in Table 1.

IDO is induced in the brain of SIV-infected monkeys exhibiting AIDS

IHC for IDO with a previously characterized mouse monoclonal antibody (Takikawa *et al*., 1988) revealed no detectable staining in sections of different brain regions of control (not shown) and SIV-infected monkeys without symptoms of AIDS (Fig. 1A). In contrast, IDO protein was found to be expressed in the brain of monkeys exhibiting AIDS. This *de novo* expression was exclusively localized to non-neuronal cells in areas of infiltrates (Fig. 1C). To demonstrate that induced IDO expression depends on IDO gene transcription, ISH with [^{35}S]-labelled cRNA antisense probes was carried out. IDO mRNA was not detectable in brain tissue sections of control (not shown) and SIV-infected animals without AIDS (Fig. 1B). IDO mRNA was induced in the brain of SIV-infected monkeys with AIDS (Fig. 1D). The message exhibited a similar distribution pattern as protein in the brain.

Induction of IDO in the brain of AIDS-diseased monkeys occurs in a subset of monocyte-derived cell population in areas of virus burden

To identify the cells in which IDO is induced, co-staining experiments were performed on brain tissue sections of AIDS-diseased animals. High-power confocal laser scanning analysis after double immunofluorescence for IDO with established brain resident cellular markers CGA, GFAP and vWF revealed that neurons, astrocytes and endothelial cells did not express IDO (Fig. 2A–C). Oligodendrocytes, choroid plexus cells and ependymal cells did not synthesize IDO (not shown). A recently characterized marker known as Iba1 was used to identify the cells of monocytic origin including macrophages and microglia (Imai *et al*., 1996). IDO biosynthesis was mainly found to be co-localized with Iba1 in and near areas of productive SIV infection, macrophage nodules and multinucleated giant cells (Figs 3A and B, and 4A–C). Confocal double immunofluorescence on adjacent sections demonstrated that IDO/Iba1-co-positive cells in nodules coincided with SIV *gp120*-positive cells co-stained for Iba1 or were in close proximity to them (Fig. 4D–F). In contrast, IDO was mostly absent from Iba1-positive ramified microglia (Fig. 4A–C).

Antiretroviral treatment reduces IDO induction in the brain

To determine the influence of viral transcription and translation on lentivirus-induced IDO biosynthesis, monkeys with high viremia and increased viral load in CSF were treated with ddI for clinical stabilization followed by lipophilic 6-Cl-ddG. Only one animal (MO89) was treated only with 6-Cl-ddG. The 6-Cl-ddG animals suffered from clinical symptoms of AIDS (SIV, +AIDS, +ddG). The biosynthesis of IDO in the brain was markedly reduced by the antiviral treatment (Fig. 1E and F), except in MO77, which showed some IDO synthesis albeit at very low levels (data not shown). The effectiveness of 6-Cl-ddG treatment on virus burden was monitored by SIV *gp120* immunostaining and by ISH for SIV transcripts. Viral burden as well as Iba1-positive mononuclear infiltrates, macrophage nodules and multinucleated giant cells were markedly reduced in the brain of 6-Cl-ddG-treated monkeys. Only in MO77 minor viral burden with some signs of productive inflammation was observed. The effects of antiviral treatment on IDO biosynthesis in relation to viral burden and mononuclear reactions in the brain are summarized in Table 1.

IDO is induced in monocytes at the blood–brain barrier in late stage of disease

The first sign of infiltration, the attachment of inflammatory cells on the endothelial surface, has been observed only in the brain of untreated AIDS-diseased monkeys. Some monocytes attached to endothelial cells expressed also IDO in the brain of AIDS-diseased monkeys (Fig. 5A and B), demonstrating IDO synthesis during infiltration through the blood–brain barrier. Apparently, these cells were truly adherent and in the progress of infiltrating into the brain as they were not washed away by the transcardial perfusion prior to or during fixation procedures. On the ventricular side there were also IDO-positive cells attached to ependymal surfaces (Fig. 5C). Both cellular phenomena were inhibited by 6-Cl-ddG.

Discussion

In this study we demonstrate that IDO was mainly induced in macrophages forming nodules and multinucleated giant cells and infiltrating monocytes in areas of SIV burden. IDO was mainly absent from diffusely distributed microglia. Induction of IDO in the brain was markedly suppressed by the treatment with 6-Cl-ddG.

The antiretroviral drug 6-Cl-ddG is a lipophilic prodrug of 2′,3′-dideoxyguanosine (Shirasaka *et al*., 1990, 1991) and passes well through the blood–brain barrier of rhesus monkeys (Hawkins *et al*., 1995). The administration of 6-Cl-ddG was found to effectively inhibit proliferation of HIV-1 (Shirasaka *et al*., 1990, 1991) and SIV *in vitro* (Fujii *et al*., 1998), and also primary proliferation of SIV in acutely infected rhesus monkeys (Fujii *et al*., 1998). In chronically SIV-infected rhesus monkeys viral load in plasma and CSF decreased during 6-Cl-ddG treatment (Fujii *et al*., 1997a). Moreover, a SIV-infected rhesus monkey with AIDS showed clinical signs of recovery during 6-Cl-ddG treatment (Fujii *et al*., 1997b). Although our experimental design was different with treatment initiation at time of increased viral load in plasma and CSF (corresponding to 'virological AIDS'), our obtained results are quite consistent with the studies by Fujii *et al.* In 6-Cl-ddG-treated rhesus monkeys brain viral burden was markedly diminished, although the animals suffered from clinical symptoms of AIDS during treatment.

IDO can be activated in the brain following systemic immune stimulation with lipopolysacharide and in the course of inflammatory CNS diseases including HIV dementia (Sardar & Reynolds, 1995). Increased activity of the kynurenine pathway via IDO induction should produce high amounts of kynurenic acid and QUIN (Stone, 1993). While kynurenic acid may be neuroprotective, QUIN is a neurotoxin. In SIV/HIV-diseased subjects QUIN levels are elevated more than kynurenic acid levels in both brain parenchyma and CSF (Heyes *et al*., 1989, 1990, 1998), suggesting a net neurotoxic effect of IDO induction.

Different cell types have been proposed as an intracerebral source of QUIN, among them endothelial cells, microglial cells, astrocytes and macrophages (Heyes *et al*., 1997; Guillemin *et al*., 1999; Hansen *et al*., 2000), but direct co-localization studies of IDO and specific cellular markers have not been performed prior to the present study. Astrocytes and microglia can release QUIN *in vitro* (Heyes *et al*., 1997; Guillemin *et al*., 1999). CNS endothelial cells express IDO during malaria infection (Hansen *et al*., 2000). Using high-resolution confocal double immunofluorescence and combination of ISH with IHC for IDO and specific cellular markers we have directly localized the site of IDO induction to cells in and near lesions containing cells with SIV, and not to other cellular loci of SIV-induced inflammation – resident microglia, astrocytes and endothelial cells – in which replicating virus is low or absent.

Interferon-γ is a potent inducer of IDO in macrophages (Takikawa *et al*., 1999). IL-1 and TNFα, known to be elevated in the retroviral-infected brain (Benveniste, 1994), are also capable of stimulating IDO synthesis (Babcock & Carlin, 2000). Thus, SIV-induced IDO biosynthesis may be both initiated and sustained by these cytokines. IDO induction may be focused to areas of SIV-infected macrophages because these cytokines are uniquely present at these sites. It is also possible that locally produced virus particles may induce IDO. Marked differences in the regulation of IDO expression have been reported between macrophages and microglial cells (Alberati-Giani *et al*., 1997). This may also explain why SIV-induced IDO biosynthesis was mainly localized to the macrophage/multinucleated giant cell compartment and did not occur globally in microglia in spite of synthesis of cytokines in both microglia and macrophages.

IDO localization to areas of virus replication implies that L-kynurenine generation is relatively focused, rather than globally activated, in the SIV-infected brain. IDO is not induced in bystander cells participating in generalized glial activation during CNS infection. As QUIN is a selective neurotoxin to cells bearing the NMDA-type glutamate receptor (Schwarcz *et al*., 1983) – how does neurodegeneration during lentiviral infection originate from these foci of IDO production and spread diffusely throughout the brain? In part this may be due to the generation of highly diffusible substances from the sites of IDO production in the brain. Activation of IDO is functionally coupled to that of inducible nitric oxide synthase (iNOS; Alberati-Giani *et al*., 1997) and iNOS is increased in areas of SIV replication (Li *et al*., 1999). iNOS and IDO expression are both up-regulated by interferon-γ (Takikawa *et al*., 1988; Melillo *et al*., 1994). Expression of iNOS results in the generation of highly diffusible NO, which may synergize with QUIN to exacerbate neuronal damage. QUIN may be generated away from the sites of IDO production by diffusion of L-kynurenine into astrocytes and microglia that can convert it to QUIN (Heyes *et al*., 1998). Finally, QUIN itself may release glutamate as a neurotoxin (Tavares *et al*., 2002), further augmenting the wide-spread neurotoxic effect of QUIN.

Our obtained results are in concordance with a recently published study by Burudi *et al*. (2002), who reported that IDO mRNA expression occurred in cells of the monocytic lineage in SIV encephalitis, and that the levels of IDO mRNA correlated with viral load and interferon-γ levels. In addition, we demonstrated here that the expression and regulation of IDO mRNA was paralleled by the actual expression of IDO in the brain of SIV-infected monkeys. Our data indicate that the observed change in protein levels is likely occurring at the transcriptional level as a transcriptome response, rather than as a post-translational response. Our new finding that IDO production is susceptible to CNS-directed antiretroviral therapy correlating with decreased brain virus burden is consistent with reports of decreased QUIN levels in CSF of patients with AIDS following highly active antiretroviral therapy (Gendelman *et al*., 1998; Look *et al*., 2000). The effects of IDO and iNOS induction at local sites of SIV replication are likely to be transmitted globally to the brain, resulting in irreversible neurodegeneration, at some point in viral disease. Strategies for therapeutic intervention in neuro-AIDS may therefore need to take into account not only the effectiveness of blocking IDO and iNOS induction, but also the stage of disease at which their global effects are irreversibly transmitted from local sites of viral replication.

Acknowledgements

This study was supported by the Volkswagen Foundation to L. E. Eiden and E. Weihe. For excellent technical work we are indebted to R. Vertesi from L. E. Eiden's lab and E. Rodenberg-Frank, M. Zibuschka, P. Sack, P. Lattermann and H. Schneider from E. Weihe's lab. Parts of this study were presented at the Cojoint Meeting of the 4th International Symposium on Neurovirology and 10th Conference on Neuroscience on HIV Infection, June 2002, Düsseldorf, Germany.

Abbreviations

6-Cl-ddG, 6-chloro-2′,3′-dideoxyguanosine; BSA, bovine serum albumin; CGA, chromogranin A; CSF, cerebrospinal fluid; ddI, 2′,3′-dideoxyinosine; GFAP, glial fibrillary acid protein; *gp120*, glycoprotein *120*; HIV, human immunodeficiency virus; Iba1, ionized calcium-adapter binding molecule; IDO, indoleamine-2,3-dioxygenase; IHC, immunohistochemistry; iNOS, inducible nitric oxide synthase; ISH, *in situ* hybridization; NMDA, *N*-methyl-D-aspartate; PBS, phosphate-buffered saline; QUIN, quinolinic acid; SIV, simian immunodeficiency virus; vWF, von Willebrand factor.

References

Abele, A.E., Scholz, K.P., Scholz, W.K. & Miller, R.J. (1990) Excitotoxicity induced by enhanced excitatory neurotransmission in cultured hippocampal pyramidal neurons. *Neuron*, **2**, 413–419.

Alberati-Giani, D., Malherbe, P., Ricciardi-Castagnoli, P., Kohler, C., Denis-Donini, S. & Cesura, A.M. (1997) Differential regulation of indoleamine 2,3-dioxygenase expression by nitric oxide and inflammatory mediators in

IFN-gamma-activated murine macrophages and microglial cells. *J. Immunol.*, **159**, 419–426.
Babcock, T.A. & Carlin, J.M. (2000) Transcriptional activation of indoleamine dioxygenase by interleukin 1 and tumor necrosis factor alpha in interferon-treated epithelial cells. *Cytokine*, **12**, 588–594.
Beal, M.F., Kowall, N.W., Swartz, K.J., Ferrante, R.J. & Martin, J.B. (1989) Differential sparing of somatostatin-neuropeptide Y and cholinergic neurons following striatal excitotoxin lesions. *Synapse*, **3**, 38–47.
Benveniste, E.N. (1994) Cytokine circuits in brain. Implications for AIDS dementia complex. *Res. Publishers Assoc. Res. Nerv. Ment.*, **72**, 71–88.
Bissel, S.J., Wang, G., Ghosh, M., Reinhart, T.A., Capuano, S. 3rd, Stefano Cole, K., Murphey-Corb, M., Piatak, M. Jr, Lifson, J.D. & Wiley, C.A. (2002) Macrophages relate presynaptic and postsynaptic damage in simian immunodeficiency virus encephalitis. *Am. J. Pathol.*, **160**, 927–941.
Block, F. & Schwarz, M. (1994) Expression of GFAP in the striatum and its projection areas in response to striatal quinolinic acid lesion in rats. *Neuroreport*, **5**, 2237–2240.
Brew, B.J., Corbeil, J., Pemberton, L., Evans, L., Saito, K., Penny, R., Cooper, D.A. & Heyes, M.P. (1995) Quinolinic acid production is related to macrophage tropic isolates. *J. Neurovirol.*, **1**, 369–374.
Budka, H. (1986) Multinucleated giant cells in the brain: a hallmark of the acquired immunodeficiency syndrome (AIDS). *Acta Neuropathol. (Berl.)*, **69**, 253–256.
Burudi, E.M., Marcondes, M.C., Watry, D.D., Zandonatti, M., Taffe, M.A. & Fox, H.S. (2002) Regulation of indoleamine 2,3-dioxygenase expression in simian immunodeficiency virus-infected monkey brains. *J. Virol.*, **76**, 12233–12241.
da Cunha, A., Rausch, D.M. & Eiden, L.E. (1995) An early increase in somatostatin mRNA expression in the frontal cortex of rhesus monkeys infected with simian immunodeficiency virus. *Proc. Natl. Acad. Sci. USA*, **92**, 1371–1375.
Dai, W. & Gupta, S.L. (1990) Molecular cloning, sequencing and expression of human interferon-γ-inducible indoleamine-2,3-dioxygenase cDNA. *Biochem. Biophys. Res. Commun.*, **168**, 1–8.
Fujii, Y., Mukai, R., Akari, H., Machida, M., Mori, K., Takasaka, M., Kojima, E., Murakami, K. & Yoshikawa, Y. (1998) Antiviral effects of 6-chloro-2′,3′-dideoxyguanosine in rhesus monkeys acutely infected with simian immunodeficiency virus. *Antivir. Chem. Chemother.*, **9**, 85–92.
Fujii, Y., Mukai, R., Mori, K., Akari, H., Otani, I., Ono, F., Kojima, E., Takasaka, M., Machida, M., Murakami, K. & Yoshikawa, Y. (1997a) Efficacy of 6-chloro-2′,3′-dideoxyguanosine (6-Cl-ddG) on rhesus macaque monkeys chronically infected with simian immunodeficiency virus (SIVmac239). *J. Acquir. Immune Defic. Syndr. Hum. Retrovirol.*, **16**, 313–317.
Fujii, Y., Mukai, R., Murayama, Y., Akari, H., Machida, M., Mori, K., Takasaka, M., Murakami, K. & Yoshikawa, Y. (1997b) Efficacy of 6-chloro-2′,3′-dideoxyguanosine (6-Cl-ddG) on an ARC/AIDS rhesus macaque (Macaca mulatta) infected with simian immunodeficiency virus. *Exp. Anim.*, **46**, 83–87.
Gendelman, H.E., Zheng, J., Coulter, C.L., Ghorpade, A., Che, M., Thylin, M., Rubocki, R., Persidsky, Y., Hahn, F., Reinhard, J. Jr & Swindells, S. (1998) Suppression of inflammatory neurotoxins by highly active antiretroviral therapy in human immunodeficiency virus-associated dementia. *J. Infect. Dis.*, **178**, 1000–1007.
Guillemin, G.J., Kerr, S.J., Smythe, G.A., Armati, P.J. & Brew, B.J. (1999) Kynurenine pathway metabolism in human astrocytes. *Adv. Exp. Med. Biol.*, **467**, 125–131.
Hansen, A.M., Driussi, C., Turner, V., Takikawa, O. & Hunt, N.H. (2000) Tissue distribution of indoleamine-2,3-dioxygenase in normal and malaria-infected tissue. *Redox Report*, **5**, 112–115.
Hawkins, M.E., Mitsuya, H., McCully, C.L., Godwin, K., Murakami, K., Poplack, D.G. & Balis, F.M. (1995) Plasma and cerebrospinal fluid pharmacokinetics of dideoxypurine nucleoside analogs in rhesus monkeys. *Antimicrob. Agents Chemother.*, **39**, 1259–1264.
Heyes, M.P., Kim, P. & Markey, S.P. (1988) Systemic lipopolysaccharide and pokeweek mitogen increase quinolinic acid content of mouse cerebral cortex. *J. Neurochem.*, **51**, 1946–1948.
Heyes, M.P., Mefford, I.N., Quearry, B.J., Dedhia, M. & Lackner, A. (1990) Increased ratio of quinolinic acid to kynurenic acid in cerebrospinal fluid of D-retrovirus *Rhesus macaques*: relationship to clinical and viral status. *Ann. Neurol.*, **27**, 666–675.
Heyes, M.P., Rubinow, D., Lane, C. & Markey, S.P. (1989) Cerebrospinal fluid quinolinic acid concentrations are increased in acquired immunodeficiency syndrome. *Ann. Neurol.*, **26**, 275–277.
Heyes, M.P., Saito, K., Chen, C.T., Proescholdt, M.G., Nowak, T.S. Jr, Li, J., Beagles, K.E., Proescholdt, M.A., Zito, M.A., Kawai, K. & Markey, S.P. (1997) Species heterogeneity between gerbils and rats: quinolinate production by microglia and astrocytes and accumulations in response to ischemic brain injury and systemic immune activation. *J. Neurochem.*, **69**, 1519–1529.
Heyes, M.P., Saito, K., Lackner, A., Wiley, C.A., Achim, C.L. & Markey, S.P. (1998) Sources of the neurotoxin quinolinic acid in the brain of HIV-1 infected patients and retrovirus-infected macaques. *FASEB J.*, **12**, 881–896.
Imai, Y., Ibata, I., Ito, D., Ohsawa, K. & Kohsaka, S. (1996) A novel gene iba1 in the major histocompatibiliy complex class III region encoding an EF hand protein expressed in a monocytic lineage. *Biochem. Biophys. Res. Commun.*, **224**, 855–862.
Kent, K.A., Rud, E., Cororan, T., Powell, C., Thiriart, C., Collignon, C. & Stott, E.J. (1992) Identification of two neutralizing and eight nonneutralizing epitopes on simian immunodeficiency virus envelope using monoclonal antibodies. *AIDS Res. Hum. Retroviruses*, **8**, 1147–1151.
Lane, J.H., Sasseville, V.G., Smith, M.O., Vogel, P., Pauley, D.R., Heyes, M.P. & Lackner, A.A. (1986) Neuroinvasion by simian immunodeficiency virus coincides with increased numbers of perivascular macrophages/microglia and intrathekal immune activation. *J. Neurovirol.*, **2**, 423–432.
Lawrence, E.M. & Major, E.O. (2002) HIV-1 and the brain: connections between HIV-1 associated dementia, neuropathology and neuroimmunology. *Mikrobes Infect.*, **4**, 301–308.
Li, Q., Eiden, L.E., Cavert, W., Reinhart, T.A., Rausch, D.M., Murray, E.A., Weihe, E. & Haase, A.T. (1999) Increased expression of nitric oxide synthase and dendritic injury in simian immunodeficiency virus encephalitis. *J. Human Virol.*, **2**, 139–145.
Lipton, S.A., Sucher, N.J., Kaiser, P.K. & Dreyer, E.B. (1991) Synergistic effects of HIV coat protein and NMDA receptor-mediated neurotoxicity. *Neuron*, **7**, 111–118.
Look, M.P., Altfeld, M., Kreuzer, K.A., Riezler, R., Stabler, S.P., Allen, R.H., Sauerbruch, T. & Rockstroh, J.K. (2000) Parallel decrease in neurotoxin quinolinic acid and soluble tumor necrosis factor receptor p75 in serum during highly active antiretroviral therapy of HIV type 1 disease. *AIDS Res. Human Retroviruses*, **16**, 1215–1221.
Luabeya, M.-K., Dallasta, L.M., Achim, C.L., Pauza, C.D. & Hamilton, R.L. (2000) Blood–brain barrier disruption in simian immunodeficiency virus encephalitis. *Neuropathol. Appl. Neurobiol.*, **26**, 454–462.
Luthert, P.J., Montgomery, M.M., Dean, A.F., Cook, R.W., Baskerville, A. & Lantos, P.L. (1995) Hippocampal neuronal atrophy occurs in rhesus macaques following infection with simian immunodeficiency virus. *Neuropathol. Appl. Neurobiol.*, **21**, 529–534.
Melillo, G., Cox, G.W., Biragyn, A., Sheffler, L.A. & Varesio, L. (1994) Regulation of nitric-oxide synthase mRNA expression by interferon-gamma and picolinic acid. *J. Biol. Chem.*, **269**, 8128–8133.
Mellor, A.L., Keskin, D.B., Johnson, T., Chandler, P. & Munn, D.H. (2002) Cells expressing indoleamine 2,3-dioxygenase inhibit T cell responses. *J. Immunol.*, **168**, 3771–3776.
Munn, D.H., Sharma, M.D., Lee, J.R., Jhaver, K.G., Johnson, T.S., Keskin, D.B., Marshall, B., Chandler, P., Antonia, S.J., Burgess, R., Slingluff, C.L. Jr & Mellor, A.L. (2002) Potential regulatory function of human dendritic cells expressing indoleamine 2,3-dioxygenase. *Science*, **297**, 1867–1870.
Murray, E.A., Rausch, D.M., Lendvay, J., Sharer, L.R. & Eiden, L.E. (1992) Cognitive and motor impairments associated with SIV infection in rhesus monkeys. *Science*, **255**, 1246–1249.
Perkins, M.N. & Stone, T.W. (1983) Pharmacology and regional variations of quinolinic acid-evoked excitations in the rat central nervous system. *J. Pharmacol. Exp. Ther.*, **226**, 551–557.
Reinhart, T.A., Rogan, M.J., Huddleston, D., Rausch, D.M., Eiden, L.E. & Haase, A.T. (1997) Simian immunodeficiency virus burden in tissues and cellular compartments during clinical latency and AIDS. *J. Infect. Dis.*, **176**, 1198–1208.
Sardar, A.M. & Reynolds, G.P. (1995) Frontal cortex indoleamine-2,3-dioxygenase activity is increased in HIV-1-associated dementia. *Neurosci. Lett.*, **187**, 9–12.
Schäfer, M.K.-H., Herman, J.P. & Watson, S.J. (1992) In situ hybridization immunohistochemistry. In London, E.D. (Ed), *Imaging Drug Action in the Brain.* CRC Press, Boca Raton, p. 337.
Schäfer, M.K.-H., Nohr, D., Romeo, H., Eiden, L.E. & Weihe, E. (1994) Panneuronal expression of chromogranin A in rat nervous system. *Peptides*, **15**, 263–279.
Schwarcz, R. & Köhler, C. (1983) Differential vulnerability of central neurons of the rat to quinolinic acid. *Neurosci. Lett.*, **38**, 85–90.

Schwarcz, R., Whetsell, W.O. Jr & Mangano, R.M. (1983) Quinolinic acid: an endogenous metabolite that produces axon-sparing lesions in rat brain. *Science*, **219**, 316–318.

Shirasaka, T., Murakami, K., Ford, H., Kelley, J., Yoshioka, H., Kojima, E., Aoki, S., Driscoll, J.S., Broder, S. & Mitsuya, H. (1990) Halogeneted congeners of 2′,3′-dideoxypurine nucleosides active against HIV in vitro: a new class of lipophilic prodrugs. *Proc. Natl. Acad. Sci. USA*, **87**, 9426–9430.

Shirasaka, T., Watanabe, K., Yoshioka, H., Kojima, E., Aoki, S., Murakami, K. & Mitsuya, H. (1991) Lipophilic 6-halo-2′,3′-dideoxypurine nucleosides: potential antiretroviral agents targeting HIV-associated neurologic disorders. In Kumar, A. (Ed.), *Advances in Molecular Biology and Targeted Treatment for AIDS.* Plenum, Washington, D.C., pp. 323–333.

Stone, T.W. (1993) Neuropharmacology of quinolinic acid and kynurenic acids. *Pharmacol. Rev.*, **45**, 309–379.

Takikawa, O., Kuroiwa. T., Yamazaki, F. & Kido, R. (1988) Mechanism of interferon-γ action: characterization of indoleamine-2,3-dioxygenase in cultured human cells induced by interferon-γ and evaluation of the enzyme-mediated tryptophan degradation in its anticellular activity. *J. Biol. Chem.*, **263**, 2041–2048.

Takikawa, O., Tagawa, Y., Iwakura, Y., Yoshida, R. & Truscott, R.J. (1999) Interferon-gamma-dependent/independent expression of indoleamine 2,3-dioxygenase. Studies with interferon-gamma-knockout mice. *Adv. Exp. Med. Biol.*, **467**, 553–557.

Tavares, R.G., Tasca, C.I., Santos, C.E., Alves, L.B., Porciuncula, L.O., Emanuelli, T. & Souza, D.O. (2002) Quinolinic acid stimulates synaptosomal glutamate release and inhibits glutamate uptake into astrocytes. *Neurochem. Int.*, **40**, 621–627.

Theilen, H. & Kuschinsky, W. (1992) Fluorescence labeling of the capillary network in rat brains. *J. Cereb. Blood Flow Metab.*, **12**, 347–350.

Weihe, E., Nohr, D., Sharer, L., Murray, E., Rausch, D.M. & Eiden, L.E. (1993) Cortical astrocytosis in juvenile rhesus monkeys infected with simian immunodeficiency virus. *Neuroreport*, **4**, 263–266.